Towards the three-dimensional structure of a sucrose isomerase from *Pseudomonas mesoacidophila* MX-45

Stéphanie Ravaud[1], Hildegard Watzlawick[2], Ralf Mattes[2], Richard Haser[1] & Nushin Aghajari[1]*

[1] *Laboratoire de BioCristallographie, Institut de Biologie et Chimie des Protéines, UMR 5086-CNRS/UCBL, "IFR 128 BioSciences Lyon-Gerland", 7 Passage du Vercors, F-69367 Lyon cedex 07, France; phone: ++ 33 4 72 72 26 33, fax: ++ 33 4 72 72 26 16, e-mail: n.aghajari@ibcp.fr*

[2] *Universität Stuttgart, Institut für Industrielle Genetik, Allmandring 31, D-70569 Stuttgart, Germany*

Abstract: The trehalulose synthase MutB from *Pseudomonas mesoacidophila* MX-45 is a member of the glycoside hydrolase family 13, although its biological function is the isomerization of sucrose to produce trehalulose and isomaltulose, with a yield of 90% of trehalulose at 20 °C and pH 5.5-6.5. Here we report and compare the structures of two crystal forms of MutB, solved to 1.8 Å and 1.6 Å resolution, respectively. This is the first reported structure of a trehalulose synthase and the second structure of a sucrose isomerase, the first one being that of the isomaltulose synthase PalI from *Klebsiella* sp. LX3. Despite important biochemical and enzymatic differences, both enzymes display quite high sequence identity and share a common fold composed of three domains: the N-terminal catalytic domain containing a modified $(\beta/\alpha)_8$-barrel, a subdomain and the C-terminal domain. A detailed structural comparison appears to be an essential approach for the understanding of differences in enzymatic properties, including product specificity.

Key words: α-amylase family, trehalulose synthase, isomerase, X-ray crystallography, structure comparison.

Abbreviations: AS, amylosucrase from *Neisseria polysaccharea*; GH, glycoside hydrolase; OGL, oligo-1,6-glucosidase from *Bacillus cereus*; PalI, isomaltulose synthase from *Klebsiella* sp. LX3; r.m.s.d., root mean square deviation; TAKA, α-amylase from *Aspergillus oryzae*.

Introduction

In the past decades, the production of isomaltulose (α-D-glucosylpyranosyl-1,6-D-fructofuranose) and trehalulose (α-D-glucosylpyranosyl-1,1-D-fructofuranose), has aroused great interest since these structural isomers of sucrose (α-D-glucosylpyranosyl-1,2-β-D-fructofuranoside) have an interesting potential as acariogenic sugar substitutes (Minami et al., 1990; Ooshima et al., 1991) and low calorie sweeteners (Goda & Hosoya, 1983; Yamada et al., 1985). At present they are widely used in health products and in the food industry. These sucrose isomers have been found in honey but only in very small quantities (Low & Sporns, 1988; Nakajima et al., 1990), hence these alternative sugars are produced on a large scale from sucrose using immobilized bacterial cells. A small range of microorganisms including *Protaminobacter rubrum*, *Enterobacter* sp. (Mattes et al., 1998), *Serratia plymuthica* NCIB 8285 (Fujii et al., 1983; MacAllister et al., 1990; Veronese & Perlot, 1998), *Erwinia rhapontici* NCPPB 1579 (Cheetham, 1984), *Klebsiella* sp. LX3 (Zhang et al., 2002), *Klebsiella* sp. (Park et al., 1992), *Klebsiella planticola* CCRC 19112 (Huang et al., 1998), *Agrobacterium radiobacter* MX-332 (Nagai-Miyata et al., 1993) and *Pseudomonas mesoacidophila* MX-45 (Miyata et al., 1992; Nagai et al., 1994), are known to be able to produce sucrose isomers due to their ability of producing the enzyme sucrose isomerase, also called sucrose mutase or α-glucosyltransferase (EC 5.4.99.11). This enzyme catalyzes the isomerization of sucrose into both isomaltulose and trehalulose as the main products with residual amounts of glucose and fructose. The enzymatic reaction is a general acid-base catalysis taking place in a two-steps reaction, namely hydrolysis of the α-1,2 glycosidic bond of sucrose followed by the formation of α-1,6 and α-1,1 bonds to form the two isomers. The reaction is initiated by the simultaneous protonation of the glycosidic bond and the nucleophilic attack of the anomeric carbon of the

* Corresponding author

glucose moiety. This leads to the formation of the covalently linked enzyme-substrate intermediate, which following can react with either a water molecule for hydrolysis or with the fructose moiety for sucrose isomers synthesis. During the isomerization step, the relative ratio of the enzyme products is determined by the structure of fructose as described in Veronese & Perlot (1998).

The product composition varies as a function of the bacterial strain (Miyata et al., 1992; Nagai-Miyata et al., 1993; Huang et al., 1998; Mattes et al., 1998; Zhang et al., 2002). Generally isomaltulose has been found to be the major product of the bacterial enzyme while trehalulose is synthesized in much lower amounts. This is also the case for the isomaltulose synthase PalI from *Klebsiella* sp. LX3, the only sucrose isomerase for which the three-dimensional structure has been solved to date (Zhang et al., 2003a). Both structural and biochemical data suggested that a unique RLDRD motif in the proximity of the PalI active site is implicated in the isomerization process and controlled the PalI product specificity (Zhang et al. 2003a,b).

However, the enzymes from two other sources, *Agrobacterium radiobacter* MX-332 (Nagai-Miyata et al., 1993) and *Pseudomonas mesoacidophila* MX-45 (Miyata et al., 1992; Nagai et al., 1994), mainly produce trehalulose (∼ 90%). Furthermore, *Pseudomonas mesoacidophila* MX-45 produces the by-products as minor components making it extremely interesting for industrial purposes.

The trehalulose synthase MutB from *Pseudomonas mesoacidophila* MX-45 has been cloned, overexpressed, purified and characterized (Ravaud et al., 2005; H. Watzlawick et al., in preparation). The mature protein consists of a single polypeptide chain with 557 amino acid residues and a molecular weight of 64 kDa.

The MutB enzyme is stable within a pH range of 5.1-6.7 and below temperatures of 40 ℃. As concerns the enzyme activity based on sucrose decomposition, the optimal pH and temperature are pH 5.8 and 40 ℃, respectively. Optimum conditions for trehalulose production are pH 5.5–6.5 at 20 ℃ with a yield of 91% for the production of trehalulose from sucrose (20–40% solution). Besides the product specificity, MutB exhibits one other remarkable difference compared to PalI, namely the effect of metal ions on enzyme activity. Amongst others, MutB is partially inhibited by Mg^{2+} but requires Ca^{2+} for stability and activity, whereas Mg^{2+} enhanced the activity of PalI and Ca^{2+} inhibited it (Nagai et al., 1994; Zhang et al., 2002). It could therefore be expected that these enzymes present different structural characteristics. The MutB enzyme has recently been crystallized in two crystal forms (Ravaud et al., 2005), and the two resulting three-dimensional structures solved to 1.8 Å and 1.6 Å resolution, respectively (this manuscript and details in S. Ravaud, H. Watzlawick, R. Haser, R. Mattes & N. Aghajari, to be submitted).

Material and methods

Purification and crystallization of MutB

The recombinant protein was purified and crystallized as described previously (Ravaud et al., 2005). Briefly MutB was overproduced by expressing the corresponding gene in *E. coli* JM109 cells harboring the plasmid pHWG315, and purified by fast protein liquid chromatography (FPLC, Amersham Biosciences) with two consecutive steps on anion-exchange columns (H. Watzlawick et al., in preparation). The purified active protein was crystallized by the hanging drop vapor diffusion method. Crystals suitable for X-ray diffraction studies were obtained after approximately one week using PEG 20000 as precipitant, and in three days using this same precipitant and L-cysteine as additive. Interestingly, the two crystal forms were obtained in the drops under both crystallization conditions.

Data collection, structure resolution and refinement

The first crystal form diffracts X-rays to 1.8 Å and belongs to the monoclinic space group $P2_1$, with unit cell parameters a = 63.7 Å, b = 85.9 Å, c = 119.7 Å and $\beta = 97.7^\circ$. The second one diffracts to 1.6 Å resolution and belongs to the triclinic space group P1, with unit cell parameters a = 63.8 Å, b = 72.0 Å, c = 82.2 Å, $\alpha = 67.4^\circ$, $\beta = 73.1^\circ$ and $\gamma = 70.8^\circ$. All data were collected on an ADSC Quantum 4 detector at the ID14-EH4 beam line at the ESRF (European Synchrotron Radiation Facility, Grenoble, France).

As described earlier (Ravaud et al., 2005) the molecular replacement method using the AMoRe program (Navaza, 2001) was employed to solve the phase problem. The three-dimensional structure of the isomaltulose synthase PalI from *Klebsiella* sp. LX3 (without water molecules) was used as a search model (Li et al., 2003; Zhang et al., 2003a). Within each structure, two protein molecules are present in the asymmetric unit.

Refinements of the models were done using the simulated annealing routine as implemented in the software CNS version 1.1 (Brünger et al., 1998), alternating with manual building using the graphics program TURBO-FRODO (Roussel & Cambillau, 1992). The refinements of the respective structures have been completed and the R factor for the structure at 1.8 Å resolution (referred to as structure 1) is 17.8% with an R_{free} of 20.6%. For the high resolution MutB structure (referred to as structure 2), these values are respectively 18.4% and 21.9%.

Sequence and structure alignment

The sequence alignment of MutB and members of the glycoside hydrolase (GH) family 13, showing the superimposition of secondary structures, was calculated with the program CLUSTALW (Thompson et al., 1994), manually modified with SEAVIEW (Galtier et al., 1996) with respect to structural similarities, and rendered using the program ESPript (Gouet et al., 2003). Figures showing the overall structures were generated with the programs GRASP (Nicholls et al., 1991) and MOLSCRIPT (Kraulis, 1991).

Accession number

The coordinates and structure factors of the MutB crystal structures 1 and 2 solved to 1.8 and 1.6 Å resolution have been deposited at the RCSB (Research Collaboratory for Structural Bioinformatics) Protein Data Bank

Table 1. Inter-molecular interactions between molecules A and B in structures 1 and 2, respectively.

Residues involved in inter-molecular contacts	Distances in structure 1 (Å)	Distances in structure 2 (Å)
Ser118-Oγ/Thr156-O	3.9	3.8
Lys119-N/Pro154-O	2.9	2.8
Lys119-N/Val155-O	3.8	3.7
Asp120-N/Val155-O	3.2	3.1
Asp120-Oδ1/Lys119-Nζ	3.1	3.0
Asp120-Oδ1/Val155-O	3.6	3.4
Asp120-Oδ1-Thr156-O	3.6	3.6
Asp120-Oδ2/Lys119-Nζ	2.7	2.7
Asp120-Oδ2/Val155-O	3.9	3.8

(PDB; http://www.rcsb.org) under the entry codes 1ZJB and 1ZJA, respectively.

Results

Structure 1

With two MutB molecules (A and B) in the asymmetric unit of crystal form 1, the final structural model consists of 9110 protein atoms and 1551 bound water molecules. Due to poor or missing electron density, residue 1 (Lys) was not inserted in the electron density map of either molecules. Moreover, side-chains for Lys133, Asp134, Glu217, Glu403 and Glu526 in molecules A and B were refined as alanines. Double conformations were found for Val72, Met86, Met94, Phe280, Thr294, Val409 and Ser497 in molecule A and Val72, Met86, Met94, Val194, Phe280, Ile484, Ser497 and Glu501 in molecule B. Also the side-chain conformations of some residues located at the surface of the protein differed between molecules A and B, namely Lys74, Lys119, Lys177, Lys242, Glu501 and Lys557. Despite these minor differences, both molecules in the asymmetric unit are quite similar with a root mean square deviation (r.m.s.d.) of 0.14 Å, calculated on the basis of all Cα atoms.

Structure 2

As for structure 1, two MutB molecules (A and B) were found in the asymmetric unit of crystal form 2 and the final structure consists of 9139 protein atoms and 1703 bound water molecules. The side-chain for residue Lys1 in molecule A as well as in molecule B was refined as glycine and residues Lys74, Lys133, Asp134, Glu217, Glu315, Glu403 and Glu526 in molecule A and Asp120, Lys133, Asp134, Lys177, Glu217, Glu315, Asp520 and Glu526 in molecule B were refined as alanines as no electron density was present after the corresponding Cβ's, indicating high disorder for those side-chains. Residues displaying double conformations were Ser9, Lys42, Val72, Met86, Met219, Phe280, Thr294, Arg358 and Ser551 in molecule A and Ser9, Val72, Met86, Met94, Phe2956 and Phe280 in molecule B. The side-chain conformations of some residues also significantly differed between molecules A and B, namely Lys119, Lys152, Lys220, Glu241, Asn261, Lys435, Glu472, Arg482 and Glu512.

As for structure 1, despite these differences, both molecules in the asymmetric unit are rather similar with an r.m.s.d. of 0.14 Å, based on all Cα atoms.

Comparison of structure 1 with structure 2

The superposition of the three-dimensional structures of structure 1 on structure 2 including all Cα atoms gives an r.m.s.d. of 0.12 Å and 0.13 Å for superposition of molecules A and B, respectively, and thus indicates two similar structures despite their distinct crystal packing. The main differences in the backbones between structures 1 and 2 are observed at: (i) the N-terminus, the electron density being clearer in structure 2; and (ii) in the region of non crystallographic contacts between molecule A and molecule B. These contacts defined by 9 inter-molecular interactions in structures 1 and 2, are overall slightly stronger in structure 2 (Table 1), where some of these differences may reflect the difference in resolution.

Overall structure

The two molecules in the asymmetric unit of each structure exhibit the same polypeptide fold organized into three domains: (i) the N-terminal catalytic domain; (ii) a small domain protruding out of it, named the subdomain; and (iii) the C-terminal domain, as defined for PalI (Zhang et al., 2003a). A ribbon presentation of one of the molecules is shown in Figure 1.

The N-terminal domain (residues 1-105, 176-478), which is sandwiched between the subdomain and the C-terminal domain, is a modified $(\beta/\alpha)_8$-barrel (TIM-barrel; Banner et al., 1975), made up of eight alternating β-sheets (Nβ1 to Nβ8) and α-helices (Nα1 to Nα8) constituting the catalytic core of the protein, commonly found in the family GH13 (the nomenclature of secondary structure elements is given in Figure 2). The major alterations are the insertions of α-helix Nα4' between Nβ4 and Nα4, α-helix Nα7' between Nβ7 and Nα7 and three additional α-helices (Nα8', Nα8", Nα8"') which protrude from the domain and connect the eighth strand Nβ8 to the eighth helix Nα8.

Residues 106-174 form the subdomain, corresponding to domain B in amylosucrase from *Neisseria polysaccharea* (AS). It is made up of one α-helix Sα1, one 3_{10}-helix η3 and three anti-parallel β-strands (Sβ1,

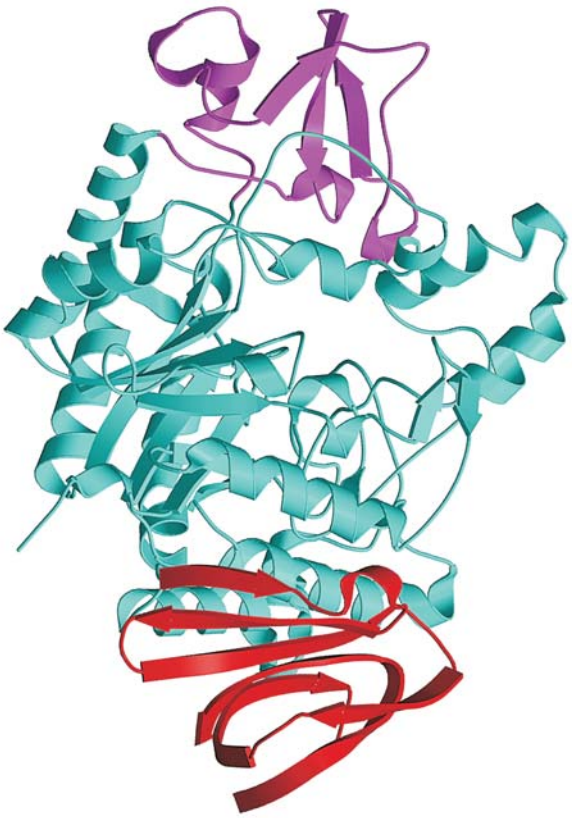

Fig. 1. The three-dimensional structure of MutB. The N-terminal catalytic domain, the subdomain and the C-terminal domain are drawn in cyan, magenta and red, respectively.

Sβ2 and Sβ3), and the remaining 70% of the 69 residues constitute loops. In α-amylases various roles have been attributed to the corresponding domain B. As concerns isozyme 2 from barley seeds, this domain has a major role in the recognition of an endogenous bifunctional inhibitor BASI (Rodenburg et al., 1994;2000; Vallée et al., 1998). Domain B has furthermore been found to play a key role in determining the overall thermostability/thermolability in a psychrophilic α-amylase from *Pseudoalteromonas haloplanctis* (Aghajari et al., 1998) and in the thermostable *Bacillus licheniformis* α-amylase (Declerck et al., 2002).

The C-terminal domain (residues 479-557) contains two antiparallel β-sheets. The inner sheet (relative to the barrel) is formed by two strands (Cβ1 and Cβ2) and the outer sheet is formed by five β-strands (Cβ3 to Cβ7). The overall surface of MutB is mostly negatively charged, especially around the active site cavity (Fig. 3). This highly negative character of the $(\beta/\alpha)_8$-barrel is characteristic of all known α-amylase three-dimensional structures, suggesting a high importance for sugar protein interactions.

Relation to glycoside hydrolase family 13 enzymes

In Figure 2 a sequence comparison of MutB with selected proteins from the α-amylase family GH13 is shown: PalI, isomaltulose synthase from *Klebsiella* sp. LX3 (Zhang et al., 2003a), OGL, oligo-1,6-glucosidase from *Bacillus cereus* (Watanabe et al., 1997), AS, amylosucrase from *Neisseria polysaccharea* (Skov et al., 2001), and TAKA, α-amylase from *Aspergillus oryzae* (Matsuura et al., 1984). It can be seen that MutB has the highest similarity to PalI, with which it displays 65.4% sequence identity, which is not surprising in that both proteins catalyze the same enzymatic reactions. Consequently, this high similarity helped to determine the MutB structure by using the molecular replacement method with the PalI structure as a search model. Two main differences are, however, observed when inspecting the primary structures of these enzymes. The first one concerns the putative isomerization motif situated in a region of MutB that shares little similarity in three-dimensional structure when compared with those of OGL, AS and TAKA. Indeed MutB contains a distinct short sequence ^{284}RYDRA^{288} (see Figure 2). The second difference occurs in the C-terminal domain, which has been suggested to contribute to the conformational stability of the overall structure and of the active site pocket in PalI (Zhang et al., 2003a).

MutB exhibits also 44.5%, 16.8% and 20.1% sequence identity with OGL, AS and TAKA, respectively. Despite of some low overall sequence identity, all five proteins display 7 well-conserved sequence regions. Four of them covering strands Nβ3, Nβ4, Nβ5 and Nβ7 of the TIM-barrel are used for defining the α-amylase family 13 (Nakajima et al., 1986; MacGregor et al., 2001). The 3 additional conserved sequence regions are more related to enzyme specificity, structure or taxonomy (Janecek, 1992; 1994a,b; 1995a). In the conserved region located near the C-terminus of the subdomain, the template sequence QPDLN, characteristic of the "oligo-1,6-glucosidase group" (Janecek, 2002; Oslancova & Janecek, 2002), is perfectly conserved in MutB, PalI and AS, but not in TAKA.

The sixth conserved region, corresponding to the strand Nβ2, is characterized in all five enzymes by a glycine residue (Gly45 in MutB) followed by 7 residues and then a conserved proline (Pro53 in MutB), again indicating that MutB indeed belongs to the α-amylase family (Janecek, 1995b).

Finally, the seventh region covering the strand Nβ8 contains the well conserved Gly359 (MutB numbering) in MutB, AS, OGL and TAKA. This is a typical feature of the "oligo-1,6-glucosidase group"(Oslancova & Janecek, 2002), which has been substituted with an alanine in PalI.

Active site

The three catalytic residues of MutB have been identified by analogy with those of PalI, OGL, AS and TAKA and thus the nucleophile is Asp200, the general acid-base residue Glu254, and the third catalytic residue Asp327 (MutB numbering). They are found re-

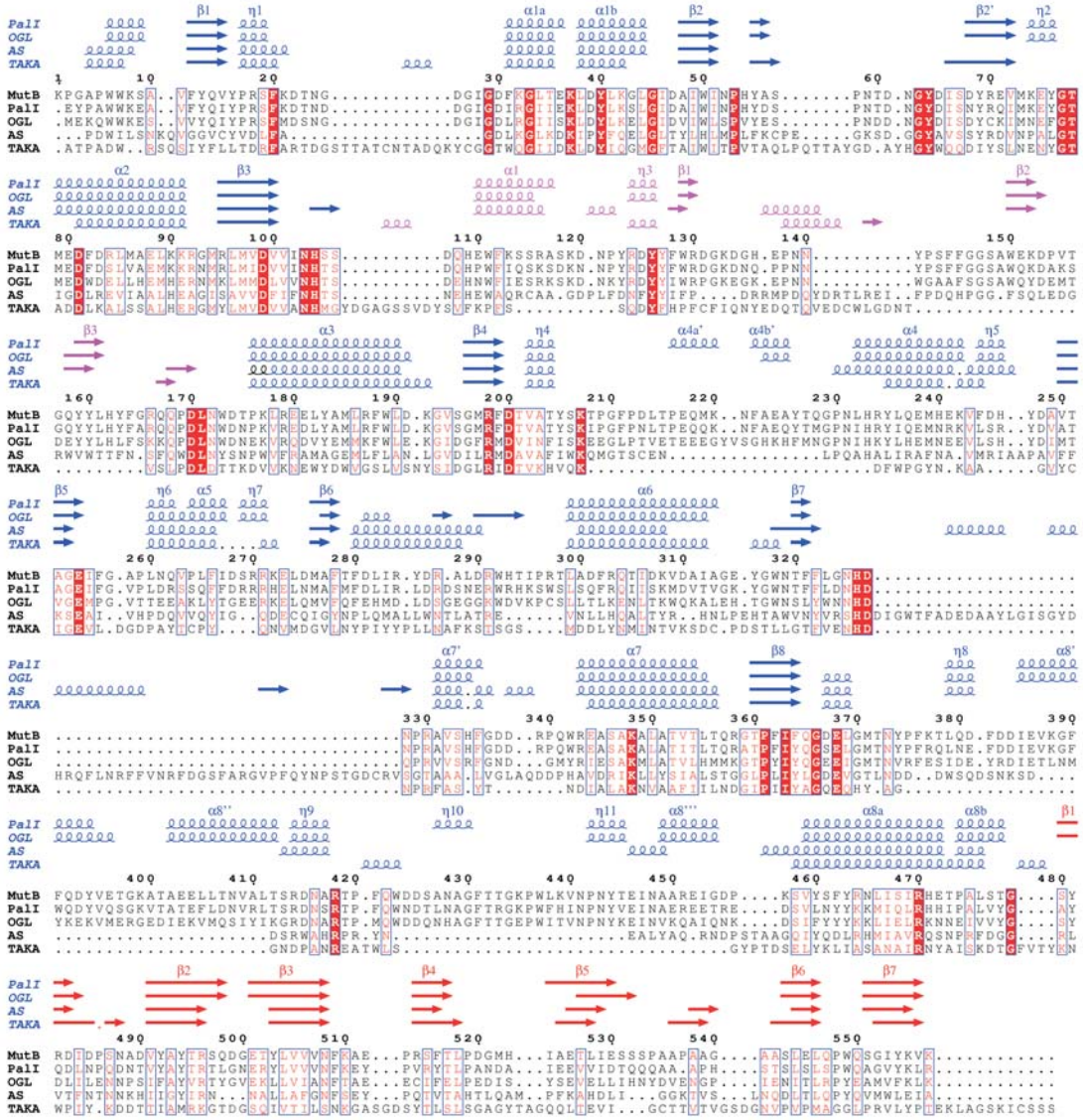

Fig. 2. Tertiary structure-based alignment between MutB and members of family GH13: PalI, isomaltulose synthase from *Klebsiella* sp. LX3 (Zhang et al., 2003a); OGL, oligo-1,6-glucosidase from *Bacillus cereus* (Watanabe et al., 1997) starting after the unique N-domain; AS, amylosucrase from *Neisseria polysaccharea* (Skov et al., 2001); TAKA, α-amylase from *Aspergillus oryzae* (Matsuura et al., 1984). Numbering corresponds to MutB and the MutB assignment of secondary structure elements, according to DSSP (Kabsch & Sander, 1983) of PalI, OGL, AS and TAKA, are inserted over the alignment, colored in blue for the N-terminal domain, in magenta for the subdomain, and in red for the C-terminal domain. Identical residues are highlighted in red and similar residues are written in red and surrounded by boxes.

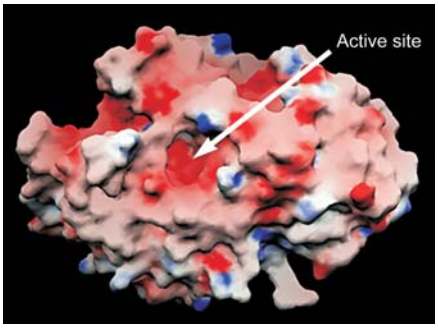

Fig. 3. Overall view of the MutB surface colored as a function of charges where positive and negative charges are presented in blue and red, respectively. The active site area is indicated in this figure.

spectively at the C-termini of strands Nβ4, Nβ5 and Nβ7 in the $(\beta/\alpha)_8$-barrel, as required for family GH13 members. The Nβ3 Asp99, the Nβ4 Arg198, and two histidine residues, His104 and His326 (MutB numbering) are also well conserved in MutB as in the other α-amylase family GH13 members.

Discussion

The three-dimensional structure of MutB from *Pseudomonas mesoacidophila* MX-45 is the first structure of a trehalulose synthase and the second one of a sucrose isomerase solved to date, the first being that of the isomaltulose synthase PalI from *Klebsiella* sp. LX3.

The present structural results confirm that MutB belongs to family GH13, which exhibits distinct enzymatic activities. Clearly MutB meets the four requirements that define the α-amylase family GH13 (Takata et al., 1992): (i) the protein acts on α-glycosidic linkages and (ii) can hydrolyse them, (iii) structure-based alignment revealed that the primary structure of MutB contains 7 well conserved regions, amongst which four of them are located in the $(\beta/\alpha)_8$-barrel and are used to identify members of the family GH13, moreover the 3 additional regions define MutB as a member of the "OGL group", and (iv) three conserved catalytic residues, namely Asp200, Glu254, Asp327 as well as 4 other conserved residues Asp99, Arg198, His104 and His326 form the active site of MutB.

MutB and PalI display important biochemical and enzymatic differences, despite a quite high sequence identity. The crystal structure of MutB described here represents the first step in a study aiming at an improved understanding of these dissimilarities and more generally of the particular product specificity of the sucrose isomerase family. The higher resolution obtained for the crystal structures of MutB (1.6 Å resolution against 2.2 Å for PalI) may allow us to perform a more detailed analysis of the molecular structure so as to identify more precisely specific features required for isomerization.

Preliminary analysis of the MutB three-dimensional structure shows that it displays a fold composed of three domains common to those reported for AS, OGL, TAKA and, more generally, to α-amylases structures. Detailed structural comparative studies appear to be an essential approach for understanding the differences in enzymatic properties between these GH13 enzymes. The fact that two crystal forms of MutB have been grown allows us to identify structural differences within the MutB system, which may be solely due to crystal packing effects.

Moreover this study requires three-dimensional structures at high resolution of various enzyme/substrate and/or inhibitor complexes to define the catalytic subsites and analyze the reaction mechanism in details. Such studies are in progress.

Structural analyses combined with rational protein engineering experiments would also be necessary in order to understand activity, substrate specificity, and product profile. Three mutants of MutB with altered activity and product specificity have already been expressed and purified and crystallization trials are underway.

Acknowledgements

Support from the CNRS (Centre National de la Recherche Scientifique) is gratefully acknowledged and we thank Xavier Robert and Patrice Gouet for help with figures.

References

Aghajari, N., Feller, G., Gerday, C. & Haser, R. 1998. Structures of the psychrophilic *Alteromonas haloplanctis* α-amylase give insights into cold adaptation at a molecular level. Structure **6:** 1503–1516.

Banner, L.W., Bloomer, A.C., Petsko, G.A., Phillips, D.C., Pogson, C.I., Wilson, I.A., Corran, P.H., Furth, A.J., Milman, J.D., Offord, R.E., Priddle, J.D. & Waley, S.G. 1975. Structure of chicken muscle triose phosphate isomerase determined crystallographically at 2.5 Å resolution using amino acid sequence data. Nature **255:** 609–614.

Brünger, A.T., Adams, P.D., Clore, G.M., DeLano, W.L., Gros, P., Grosse-Kunstleve, R.W., Jiang, J.S., Kuszewski, J., Nilges, M., Pannu, N.S., Read, R.J., Rice, L.M., Simonson, T. & Warren, G.L. 1998. Crystallography & NMR system: A new software suite for macromolecular structure determination. Acta Cryst. **D54:** 905–921.

Cheetham, P.S. 1984. The extraction and mechanism of a novel isomaltulose-synthesizing enzyme from *Erwinia rhapontici*. Biochem J. **220:** 213–220.

Declerck, N., Machius, M., Joyet, P., Wiegand, G., Huber, R. & Gaillardin, C. 2002. Engineering the thermostability of *Bacillus licheniformis* α-amylase. Biologia, Bratislava **57 (Suppl. 11):** 203–211.

Fujii, S., Kishihara, S., Komoto, M. & Shimizu, J. 1983. Isolation and characterization of oligosaccharides produced from sucrose by transglucosylation action of *Serratia plymuthica*. Nippon Shokuhin Kogyo Gakkaishi **30:** 339–334.

Galtier, N., Gouy, M. & Gautier, C. 1996. SeaView and Phylo_win, two graphic tools for sequence alignment and molecular phylogeny. Comput. Applic. Biosci. **12:** 543–548.

Goda, T. & Hosoya, N. 1983. Hydrolysis of palatinose by rat intestinal sucrase-isomaltase complex. J. Jpn. Soc. Food Sci. **36:** 169–173.

Gouet, P., Robert, X. & Courcelle, E. 2003. ESPript/ENDscript: extracting and rendering sequence and 3D information from atomic structures of proteins. Nucleic Acids Res. **31:** 3320–3323.

Huang, J.H., Hsu, L.H. & Suc, J.C. 1998. Conversion of sucrose to isomaltulose by *Klebsiella planticola* CCRC 19112. J. Ind. Microbiol. Biotechnol.**21:** 22–27.

Janecek, S. 1992. New conserved amino acid region of α-amylases in the third loop of their $(\beta/\alpha)_8$-barrel domains. Biochem. J. **288:** 1069–1070.

Janecek, S. 1994a. Parallel β/α-barrels of α-amylase, cyclodextrin glycosyltransferase and oligo-1,6-glucosidase versus the barrel of β-amylase: evolutionary distance is a reflection of unrelated sequences. FEBS Lett. **353:** 119–123.

Janecek, S. 1994b. Sequence similarities and evolutionary relationships of microbial, plant and animal α-amylases. Eur. J. Biochem.**224:** 519–524.

Janecek, S. 1995a. Close evolutionary relatedness among functionally distantly related members of the $(\alpha/\beta)_8$-barrel glycosyl hydrolases suggested by the similarity of their fifth conserved sequence region. FEBS Lett. **377:** 6–8.

Janecek, S. 1995b. Tracing the evolutionary lineages among α-amylases and cyclodextrin glycosyltransferases: the question of so-called "intermediary" enzymes. Biologia, Bratislava **50:** 515–522.

Janecek, S. 2002. How many conserved sequence regions are there in the α-amylase family? Biologia, Bratislava **57 (Suppl 11):** 29–41.

Kabsch, W. & Sander, C. 1983. Dictionary of protein secondary structure: pattern recognition of hydrogen-bonded and geometrical features. Biopolymers **22:** 2577–2637.

Kraulis, P.J. 1991. MOLSCRIPT: a program to produce both detailed and schematic plots of protein structures. J. Appl. Cryst. **24:** 946–950.

Li, N., Zhang, D., Zhang, L.H. & Swaminathan, K. 2003. Expression, crystallization and preliminary X-ray analysis of

isomaltulose synthase (PalI) from *Klebsiella* sp. LX3. Acta Cryst. **D59:** 150–151.

Low, N.H. & Sporns, P. 1988. Analysis and quantification of minor di- and trisaccharides in honey using capillary gas chromatography. J. Food Sci. **53:** 558–561.

MacAllister, M., Kelly, C.T., Doyle, E. & Fogarty, W.M. 1990. The isomaltulose-synthesizing enzyme of *Serratia plymuthica*. Biotechnol. Lett. **12:** 667–672.

MacGregor, E.A., Janecek, S. & Svensson, B. 2001. Relationship of sequence and structure to specificity in the α-amylase family of enzymes. Biochim. Biophys. Acta **1546:** 1–20.

Matsuura, Y., Kusunoki, M., Harada, W. & Kakudo, M. 1984. Structure and possible catalytic residues of Taka-amylase A. J. Biochem. **95:** 697–702.

Mattes, R., Klein, K., Schiweck, H., Kunz, M. & Munir, M. 1998. DNA's encoding sucrose isomerase and palatinase. U.S. Patent 5786140.

Minami, T., Fujiwara, T., Ooshima, T., Nakajima, Y. & Hamada, S. 1990. Interaction of structural isomers of sucrose in the reaction between sucrose and glucosyltransferases from mutans streptococci. Oral Microbiol. Immunol. **5:** 189–194.

Miyata, Y., Sugitani, T., Tsuyuki, K., Ebashi, T. & Nakajima, Y. 1992. Isolation and characterization of *Pseudomonas mesoacidophila*-producing trehalulose. Biosci. Biotechnol. Biochem. **56:** 1680–1681.

Nagai-Miyata, J., Tsuyuki, K., Sugitani, T., Ebashi, T. & Nakajima, Y. 1993. Isolation and characterization of a trehalulose-producing strain of *Agrobacterium*. Biosci. Biotechnol. Biochem. **57:** 2049–2053.

Nagai, Y., Sugitani, T. & Tsuyuki, K. 1994. Characterization of α-glucosyltransferase from *Pseudomonas mesoacidophila* MX-45. Biosci. Biotechnol. Biochem. **58:** 1789–1793.

Nakajima, R., Imanaka, T. & Aiba, S. 1986. Comparison of amino acid sequences of eleven different α-amylases. Appl. Microbiol. Biotechnol. **23:** 355–360.

Nakajima, Y., Sugitani, T., Tanaka, M. & Fujii, S. 1990. Occurrence of trehalulose, 1-O-α-D-glucopyranosyl-D-fructose, in nectar honey. Nippon Shokuhin Kogyo Gakkaishi **37:** 554–558.

Navaza, J. 2001. Implementation of molecular replacement in AMoRe. Acta Cryst. **D57:** 1367–1372.

Nicholls, A., Sharp, K.A. & Honig, B. 1991. Protein folding and association: insights from the interfacial and thermodynamic properties of hydrocarbons. Proteins **11:** 281–296.

Ooshima, T., Izumitani, A., Minami, T., Fujiwara, T., Nakajima, Y. & Hamada, S. 1991. Trehalulose does not induce dental caries in rats infected with mutans streptococci. Caries Res. **25:** 277–282.

Oslancova, A. & Janecek, S. 2002. Oligo-1,6-glucosidase and neopullulanase enzyme subfamilies from the α-amylase family defined by the fifth conserved sequence region. Cell. Mol. Life Sci. **59:** 1945–1959.

Park, Y.K., Uekane, R.T. & Pupin, A.M. 1992. Conversion of sucrose to isomaltulose by microbial glucosyltransferase. Biotechnol. Lett. **14:** 547–551.

Ravaud, S., Watzlawick, H., Haser, R., Mattes, R. & Aghajari, N. 2005. Expression, purification, crystallization and preliminary X-ray crystallographic studies of the trehalulose synthase MutB from *Pseudomonas mesoacidophila* MX-45. Acta Cryst. **F61:** 100–103.

Rodenburg, K.W., Juge, N., Søgaard, M., Guo, X., Chaix, J.C. & Svensson, B. 1994. Domain B protruding at the third β-strand of the α/β-barrel in barley α-amylase confers distinct isozyme-specific properties. Eur. J. Biochem. **221:** 277–284.

Rodenburg, K.W., Vallee, F., Juge, N., Aghajari, N., Guo, X., Haser, R. & Svensson, B. 2000. Specific inhibition of barley α-amylase 2 by barley α-amylase/subtilisin inhibitor depends on charge interactions and can be conferred to isozyme 1 by mutation. Eur. J. Biochem. **267:** 1019–1029.

Roussel, A. & Cambillau, C. 1992. TURBO-FRODO. Biographics, AFMB, Marseille, France.

Skov, L.K., Mirza, O., Henriksen, A., De Montalk, G.P., Remaud-Simeon, M., Sarcabal, P., Willemot, R.M., Monsan, P. & Gajhede, M. 2001. Amylosucrase, a glucan-synthesizing enzyme from the α-amylase family. J. Biol. Chem. **276:** 5273–5278.

Takata, H., Kuriki, T., Okada, S., Takesada, Y., Iizuka, M., Minamiura, N. & Imanaka, T. 1992. Action of neopullulanase. Neopullulanase catalyses both hydrolysis and transglycosylation at α(1-4) and α(1-6) glucosidic linkages. J. Biol. Chem. **267:** 18447–18452.

Thompson, J.D., Higgins, D.G. & Gibson, T.J. 1994. CLUSTAL W: improving the sensitivity of progressive multiple sequence alignment through sequence weighting, position-specific gap penalties and weight matrix choice. Nucleic Acids Res. **22:** 4673–4680.

Vallee, F., Kadziola, A., Bourne, Y., Juy, M., Rodenburg, K.W., Svensson, B. & Haser, R. 1998. Barley α-amylase bound to its endogenous protein inhibitor BASI: crystal structure of the complex at 1.9 Å resolution. Structure **6:** 649–59.

Veronese, T. & Perlot, P. 1998. Proposition for the biochemical mechanism occurring in the sucrose isomerase active site. FEBS Lett. **441:** 348–352.

Yamada, K., Shinhara, H. & Hosoya, N. 1985. Hydrolysis of α-1-O-α-D-glucopyranosyl-D-fructofuranose (trehalulose) by rat intestinal sucrase-isomaltase complex. Nutr. Rep. Int. **32:** 1211–1222.

Zhang, D., Li, X. & Zhang, L.H. 2002. Isomaltulose synthase from *Klebsiella* sp. strain LX3: gene cloning and characterization and engineering of thermostability. Appl Environ. Microbiol. **68:** 2676–2682.

Zhang, D., Li, N., Lok, S.M., Zhang, L.H. & Swaminathan, K. 2003a. Isomaltulose synthase (PalI) of *Klebsiella* sp. LX3. Crystal structure and implication of mechanism. J. Biol. Chem. **278:** 35428–35434.

Zhang, D., Li, N., Swaminathan, K. & Zhang, L.H. 2003b. A motif rich in charged residues determines product specificity in isomaltulose synthase. FEBS Lett. **534:** 151–155.

Watanabe, K., Hata, Y., Kizaki, H., Katsube, Y. & Suzuki, Y. 1997. The refined crystal structure of *Bacillus cereus* oligo-1,6-glucosidase at 2.0 Å resolution: structural characterization of proline-substitution sites for protein thermostabilization. J. Mol. Biol.**269:** 142–153.

Received December 01, 2004
Accepted April 11, 2005